

Influence of Spatial and Temporal Laser Beam Smoothing on Stimulated Brillouin Scattering in Filamentary Laser Light

R. L. Berger, B. F. Lasinski, A. B. Langdon, T. B. Kaiser, B. B. Afeyan, B. I. Cohen, C. H. Still, and E. A. Williams

Lawrence Livermore National Laboratory, Livermore, California 94550

(Received 17 January 1995; revised manuscript received 16 May 1995)

Three-dimensional simulations are presented which calculate the time-dependent, self-consistent evolution of filamentation and stimulated Brillouin backscatter (SBBS) in nonuniform laser beams with intense hot spots. The simulations show significant reflectivity ($>1\%$) for modest average-intensity gain exponents (5–10). Many hot spots cooperate to produce a total SBBS amplification that increases with the plasma length as well as hot-spot length. Temporal beam smoothing with bandwidth comparable to the SBBS growth rate substantially reduces the nonuniform-laser-beam reflectivity.

PACS numbers: 52.35.Nx, 52.40.Db, 52.40.Nk

A number of experiments [1] have shown that the stimulated Brillouin backscattering (SBBS) reflectivity is sensitive to the laser beam “smoothness” as well as the parameters that directly influence the growth rate and gain exponent, such as the spatially averaged laser intensity I_0 , electron temperature T_{e0} , electron density n_{e0} , ion temperature, charge state Z , and atomic number A . Near the focus of a typical high-power laser beam, the intensity is very nonuniform and is characterized by speckles, diffraction limited hot spots [2] of typical width $\ell_{\perp} = f\lambda_0$ and length $\ell_s = 8f^2\lambda_0$. Here f is the f number and λ_0 is the laser wavelength. In this Letter, we show that the SBBS is amplified by the combined effects of many hot spots and that temporal beam smoothing can reduce the reflectivity nearly to uniform laser beam levels.

Since, without temporal smoothing, the spatial location of the speckles is constant, SBBS and other parametric instabilities grow preferentially in these long, narrow regions (see Fig. 1). For this reason, stimulated Brillouin scattering (SBS) is more strongly peaked in the backscattered direction than the uniform-intensity spatial or temporal growth rate can account for. One might also argue the SBBS and filamentation interaction lengths will be limited to the speckle length, since the transverse locations of the speckles are uncorrelated over distances of this order. We found this to describe filamentation correctly [3]; however, SBS is not so localized because the backscattered light is preferentially amplified if the phases of the different Fourier modes match their hot spots to those of the incident light, i.e., phase conjugation develops [4]. Temporal beam smoothing has the effect of changing the hot-spot locations on the laser bandwidth time scale because the relative phases between the “beamlets” from each phase plate element are changing. Thus one expects that temporal smoothing will weaken SBBS, since the acoustic waves, responsible for scattering and refracting the laser light, must be regenerated at a new location with a different phase relation to the incident and scattered light. This expectation is borne out by our simulations.

In addition, the speckles can create density troughs via the ponderomotive force (or pressure gradients from

nonuniform heating) that refract and intensify the laser light; in short, filamentation may occur and compete with or enhance SBS. When the SBBS is produced by the cooperative effect of many speckles, filamentation could reduce phase conjugation and perhaps SBBS. In the results presented here, SBBS, because of its faster temporal and spatial growth rates, has the effect of limiting filamentation.

Previously, the interaction of SBS and filamentation has been considered for the case of a single spot [5–7]. The results of Refs. [5] and [6] rely on strong damping of the acoustic wave. In the initial growth phase of a convective instability, the validity of strong damping requires the damping rate be greater than the growth rate, i.e., $\nu_a > \gamma_0$. The growth rate,

$$\begin{aligned} \frac{\gamma_0}{\omega_a} &= \frac{1}{4} \frac{v_0}{v_e} \frac{\omega_{pe}}{\omega_0} \left(\frac{\omega_0}{\omega_a} \right)^{1/2} \\ &= 0.3 \left(\frac{\lambda_0}{0.351 \mu\text{m}} \right)^2 \sqrt{\frac{I_0}{2 \times 10^{15} \text{ W/cm}^2} \frac{n_{e0}}{10^{21} \text{ cm}^3}} \\ &\quad \times \left(\frac{3 \text{ keV}}{T_{e0}} \right)^{3/4} \left(\frac{A}{2Z} \right)^{1/4}, \end{aligned} \quad (1)$$

is larger than the damping rate in many cases of particular interest, for example, carbon-hydrogen plasmas [8] where $\nu_a/\omega_a \sim 0.1$. Here, ω_a is the acoustic frequency, v_0 is the jitter velocity of an electron in the laser electric

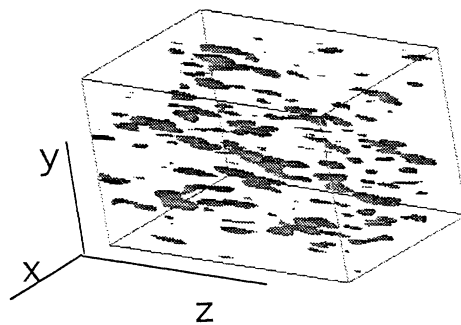


FIG. 1. Plots of surfaces of laser intensity $I = 4.5I_0$ near the focus of an $f/4$ lens for $L_x = L_y = 80\lambda_0$ and $L_z = 515\lambda_0$.

field, v_e is the electron thermal velocity, ω_{pe} is the electron plasma frequency, and ω_0 is the laser frequency. Single-species plasmas have even smaller damping rates when $ZT_e/T_i > 2$. The approach of Amin *et al.* [7], who numerically solved in 2D the light-wave equation coupled to a linearized ion-acoustic-wave equation, was not so restricted, but their approach is unsuitable for problems with a large number of hot spots with time-varying intensities because resolving the laser wavelength is incompatible with large systems. Our approach to the problem of scattering in long, narrow hot spots is to separate the acoustic wave response into short wavelength modes responsible for SBBS and into longer wavelength ones responsible for filamentation. By including a large number of hot spots in the transverse and axial directions, we can address the importance of cooperative scattering from many hot spots which the single spot simulations do not address. Most importantly, we can treat the effect of beam smoothing on SBBS, which was the primary motivation for this work.

For SBBS driven by a uniform laser beam in a uniform plasma, the steady-state reflectivity is expected to be a function of the SBBS intensity gain exponent,

$$G = \frac{1}{8} \frac{v_0^2}{v_e^2} \frac{n_e}{n_c} \frac{\omega_a}{\nu_a} \frac{\omega_0 L}{c} \\ = 12 \left(\frac{I_0}{2 \times 10^{15} \text{ W/cm}^2} \right) \left(\frac{3 \text{ keV}}{T_e} \right) \left(\frac{n_e}{1 \times 10^{21} \text{ cm}^{-3}} \right) \\ \times \left(\frac{0.3}{\nu_a/\omega_a} \right) \left(\frac{\lambda_0}{0.351 \text{ } \mu\text{m}} \right)^3 \left(\frac{L}{1 \text{ mm}} \right) \quad (2)$$

(appropriate for $n_e/n_c \ll 1$ and $T_i \ll ZT_e$), provided the threshold for absolute instability is not exceeded. Note that the same value of G is obtained with different combinations of I_0 , ν_a , and L . Recent work [6] has suggested that the gain exponent per speckle G_{hot} [set $L = 7.2 f^2 \lambda_0$ in Eq. (2)] is an important parameter in determining the reflectivity. The onset of strong reflectivity in this theory occurs for $G_{\text{hot}} = 1$ and should not depend on the plasma length or the plasma damping if G_{hot} is constant. In our simulations we also observe an f -number dependent onset of strong reflectivity (see Fig. 2) but find that it cannot be characterized by the single parameter G_{hot} as we will discuss shortly.

The incident light wave is assumed to obey a modified paraxial equation for the electric field amplitude, E_0 , of the form [9]

$$\left(\frac{\partial}{\partial t} + v_g \frac{\partial}{\partial z} - \frac{ic^2 k_0 \nabla_{\perp}^2}{\omega_0 (k_0 + \sqrt{k_0^2 - \nabla_{\perp}^2})} + \nu + \frac{1}{2} v_g' \right) E_0 \\ = \frac{-i}{2\omega_0} \frac{4\pi e^2}{m_e} (\delta n_f E_0 + \delta n_b E_i), \quad (3)$$

where $v_g = c^2 k_0 / \omega_0$ is the light wave group velocity in the z direction, ν is the collisional absorption rate, and $k_0 = \sqrt{1 - n_0/n_c} \omega_0 / c$ is the local wave number. As usual, e , m_e , c , and n_c are the electron charge, the

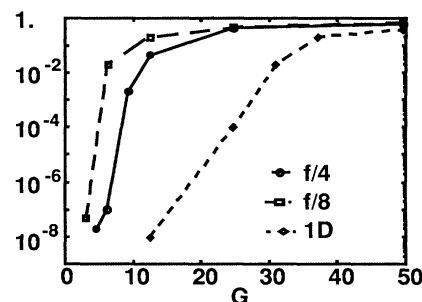


FIG. 2. Time-averaged SBS reflectivity vs G [Eq. (2)] for a uniform laser beam, a one-color $f/4$ beam, and a one-color $f/8$ beam.

electron mass, the speed of light, and the critical density, respectively. The reflected light wave obeys an equation like Eq. (2) with $v_g \rightarrow -v_g$, $E_0 \rightarrow E_i$, and $\delta n_b \rightarrow \delta n_b^*$. The backscattered light wave is treated with a boundary condition such that the flux incident on the boundary at $z = L$ is equal to the blackbody flux at the background electron temperature T_{0e} . We estimate that this flux over a spectral width of 200 nm into the solid angle of an $f/4$ lens is $\sim 10^{-13}$ of an incident laser flux of $\sim 10^{15}$ W/cm².

The low frequency acoustic wave perturbations have been decomposed into modes, δn_f , whose main variation is perpendicular to the laser propagation direction as appropriate for filamentation and SBBS modes. The SBBS acoustic wave satisfies the equation

$$\left[\frac{\partial^2}{\partial t^2} + 2\nu_a \frac{\partial}{\partial t} - C_a^2 \nabla^2 \right] n_a = Zn \frac{m_e}{8m_i} \nabla^2 a_0 a_1^*, \quad (4)$$

where the ion acoustic sound speed $C_a = [(ZT_e + \gamma_i T_i)/m_i]^{1/2}$, γ_i is $\frac{5}{3}$ or 3 as appropriate, m_i is the ion mass, and $a_{0,1} = (eE_{0,1}/m_e \omega_0) \exp(\pm ik_0 z)$. The equations are solved with a grid coarser than a light wavelength along the z direction, because the fast phase variation at $2k_0$ on the right hand side of Eq. (4) is eliminated by expanding the density perturbation n_a as $n_a = \delta n_b \exp(2ik_0 z) + \text{c.c.}$, which introduces terms proportional to $2k_0 C_a(z)$ and smaller terms proportional to its derivatives. Because no approximation is made to the frequency dependence of n_a , strongly coupled SBBS is correctly computed. The SBBS-driven acoustic wave amplitude δn_b is maintained with a source such that, in the limit that the laser field is zero, the fluctuations are at the thermal equilibrium level. The equations describing the low frequency response of the plasma to filamentation have been described elsewhere [3,10]. It is worth noting that SBBS (because it grows faster than filamentation), beam smoothing, or both obviated any need to artificially limit the density perturbation δn_f in these simulations.

No nonlinear limits were imposed on the SBS acoustic wave amplitude, which approached the wave-breaking limit and trapping amplitude in some small regions of plasma for the highest gain exponents. Simulations where we kept $|\delta n_b/n| \leq 0.1$, to model a trapping or wave-breaking limit, did not produce much reduction in

reflectivity. That is, the laser depleted spatially over a longer distance but the overall reflectivity stayed nearly constant for large systems. However, our purpose here is not to compute the experimentally observed reflectivities but to illustrate the influence of beam smoothing on SBBS. Limits on the magnitude of δn_b do allow filamentation to compete with SBBS, since the spatial growth rates may then become comparable. These subjects will be explored in more detail in a subsequent publication.

The incident laser field at $z = 0$ is specified as the sum over an array of beamlets that represent the contribution from a given portion of the lens over which the phase is constant in space, e.g., for a given RPP element. In Fig. 1, we show a plot of surfaces within which the laser intensity exceeds $4.5I_0$ for a numerically generated laser beam in the focal plane of a $f/4$ lens. In the direction of propagation, z axis, the speckles are 32 ($8f$) times longer than they are wide, which would be apparent if the scales for the x - y and z axes were the same. The isolation and the size variation of the very intense spots are apparent. The bandwidth $\Delta\omega$ is added to the model by making the overall phase $\phi(t)$ a random function of time. If the bandwidth is combined with a dispersive element, SSD is obtained [11], and the hot spots dance around on the coherence time scale. A time-varying speckle pattern is also produced if laser beams, whose frequencies ω_j differ slightly, intersect at different angles. An example is the four-color scheme implemented on Nova [12], in which each quadrant of the focusing lens had a different frequency ω_j . Bandwidth can be added to each frequency and SSD added to each quadrant. Four colors alone does not smooth as effectively as SSD on the long time scale, because the speckle pattern repeats [13] after a time $2\pi/\Delta\omega_c$, where $\Delta\omega_c = \text{Min}|\omega_j - \omega_j'|$. With solid-state laser systems, the laser bandwidth needed for temporal smoothing is limited to $<0.1\%$ if the frequency is to be doubled and $<0.03\%$ if the frequency is to be tripled with good efficiency.

We compare the effectiveness of the different temporal schemes in reducing SBBS. The temporal smoothing effects on filamentation will be discussed in a separate publication. We concentrate on simulations in uniform, low- Z plasmas with $n_{0e} = 0.1n_c$, $T_{0e} = 3$ keV, $\lambda_0 = 0.351 \mu\text{m}$, $I_0 \sim (0.5-4) \times 10^{15}$, $f \sim 4-8$, $\Delta\omega_c = (4-8) \times 10^{-4}$, $\Delta\omega = (2.5-15) \times 10^{-4}$, and $\nu_a/\omega_a = 0.05-0.2$. These parameters are representative of recent laser plasma experimental parameters [14-16] and are expected to remain of interest for ignition scale plasmas [17]. In Fig. 2, the SBS reflectivity as a function of G [Eq. (2)] is displayed for $f/4$ and $f/8$ without any temporal smoothing for $\nu_a/\omega_a = 0.1$ and a fixed length along the propagation direction of $515\lambda_0$. Note that the onset of strong reflectivity is a function of f number but not the f^2 scaling one expects for a gain exponent that depends on the speckle length. The onset starts at a gain exponent of 8 for $f/4$ ($G_{\text{hot}} = 2$) and 6 for $f/8$ ($G_{\text{hot}} = 6$). The $f/8$ reflectivity is systematically

larger for the same plasma conditions and laser intensity. Because filamentation did not play a role for $f/4$, whereas, above 10^{15} W/cm^2 , it does for $f/8$, some of the differences between $f/4$ and $f/8$ simulations may be the result of some filamentation in the $f/8$ simulations. $f/8$ simulations in which the light refraction was neglected (but the hot spots remained) showed about a factor of 2 decrease in reflectivity at gain exponents of 12. This does not account for the entire difference between $f/4$ and $f/8$, so the higher gain per speckle for $f/8$ than $f/4$ is probably also playing a role. Although the reflectivity as a function of gain exponent is similar for other damping rates, its value is systematically larger for smaller damping rates. Rather than pursuing this subject further, we concentrate on the effects of temporal beam smoothing.

The laser bandwidth available at $0.35 \mu\text{m}$ on Nova is too small to directly reduce the amplification or growth rate. However, in multidimensional, many-speckle simulations, temporal smoothing has the important effect of changing the characteristic gain that SBBS experiences since, on the time scale it takes a scattered light wave to grow to saturation, the acoustic wave responsible for scattering the laser light must grow in a new location. Acoustic waves are highly localized because, undriven, they spatially damp over a few light wavelengths. In Fig. 3, the reflectivity is displayed as a function of gain exponent for $f/4$ illumination with and without beam smoothing. The results for one color, four color, SSD with bandwidth $\Delta\omega/\omega_0 = 4 \times 10^{-4}$ and 1.5×10^{-3} , and a combination of four color and SSD with $\Delta\omega/\omega_0 = 2.5 \times 10^{-4}$ are shown. The color separation was chosen as appropriate for Nova experiments, namely, $\Delta\omega_c/\omega_0 = 4 \times 10^{-4}$. All the reflectivities shown in Fig. 3 are far in excess of levels produced by bremsstrahlung emission or the Thomson scattering from thermal ion acoustic fluctuations. The Thomson scattering reflectivity in these simulations is 2×10^{-9} . Below gain exponents of 10, the effect of beam smoothing is quite dramatic; the reflectivities drop below 10^{-6} for gain exponents $G \leq 10$. The

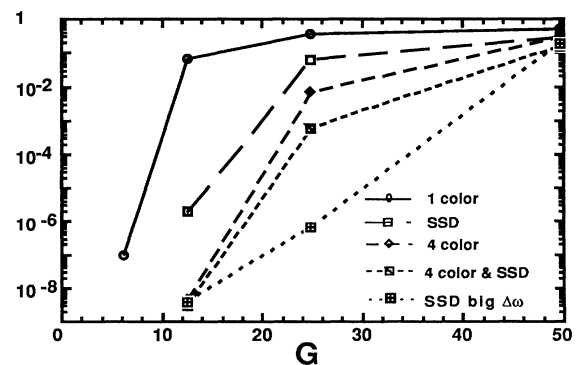


FIG. 3. Time-averaged $f/4$ SBS reflectivity vs 1D convective gain exponent for a one-color beam, an SSD beam with bandwidth $\Delta\omega = 4 \times 10^{-4}\omega_0$, a four-color beam, a four-color beam with SSD bandwidth $\Delta\omega = 2.5 \times 10^{-4}\omega_0$, and an SSD beam with bandwidth $\Delta\omega = 1.5 \times 10^{-3}\omega_0$.

SBBS growth rate for the simulations at $G = 12.5$ (computed with the average intensity $I = 2 \times 10^{15}$ W/cm²) is $7.5 \times 10^{-4} \omega_0$, which exceeds the small bandwidth SSD and the line separation for four colors. Nonetheless, there is still a reduction in reflectivity. The combination of four colors and only 2.5×10^{-4} SSD brings the reflectivity significantly below the four color without SSD because the hot-spot locations are no longer periodic in time. SSD with 1.5×10^{-3} bandwidth is by far the most effective in reducing the SBBS; the reflectivity drops to a level 3 orders of magnitude below the four color with SSD scheme. Thus a few lines with a span of frequency, $\omega_{\max} - \omega_{\min}$, is no substitute for real bandwidth with the same frequency span. With much larger gain exponents, $G = 50$ (laser intensity $= 4 \times 10^{15}$ W/cm²), all the reflectivities are greater than 20%, but that should be expected, since the reflectivity for a uniform laser beam at this intensity and G is 35%.

A number of other $f/4$ simulations have been done with different damping rates, plasma lengths, and laser intensities. At $G = 12$, the small bandwidth SSD reflectivities for different simulations vary by 5 orders of magnitude with the highest reflectivity of 1.8% at the highest intensity 4×10^{15} W/cm², $L = 515\lambda_0$, and $\nu_a/\omega_a = 0.2$, the lowest reflectivity of 2×10^{-7} at the lowest intensity of 1×10^{15} W/cm², $L = 515\lambda_0$, and $\nu_a/\omega_a = 0.05$. Increasing the intensity by a factor of 2 and halving the length to keep G constant also results in higher reflectivity. These results support the idea that the smoothing must be done on the growth rate time scale to be effective. The reflectivity increases 2 orders of magnitude from 2×10^{-6} to 2×10^{-4} by increasing the damping ν_a/ω_a from 0.05 to 0.1 to 0.2 and the length from $256\lambda_0$ to $515\lambda_0$ to $1030\lambda_0$. These results are displayed in Fig. 4. Both of these trends with length and intensity make sense if the addition of the SSD bandwidth increased the effective acoustic wave damping to a value as large as $0.2\omega_a$ so that the gain exponent is increasing with L and/or intensity I . This appears plausible because $\Delta\omega_{\text{SSD}}/\omega_0 = 4 \times 10^{-4}$, whereas $\nu_a/\omega_0 \cong 2(\nu_a/\omega_a) \times 10^{-3} = 10^{-4}$ at the lowest damping rate. $f/8$ simulations with $G = 12.5$ and $L = 515\lambda_0$, also shown in Fig. 4, display a similar trend to the $f/4$ simulations but with much higher reflectivities.

Our 3D simulations have probed the influence of laser light nonuniformity on the level of near backscattered Brillouin light with the self-consistent evolution of filamentation. The role of temporal smoothing in reducing the level of SBS has been demonstrated theoretically for the first time. This work provides a basis for understanding when temporal smoothing will be very effective in reducing SBBS [1] and when it will be less so [15,16].

We are indebted to S. Dixit and D. Eimerl for valuable discussions about beam smoothing techniques and to S. W. Haan, W. L. Kruer, J. D. Lindl, R. L. Kauffman, J. D. Kilkenny, B. J. MacGowan, L. V. Powers, and M. D.

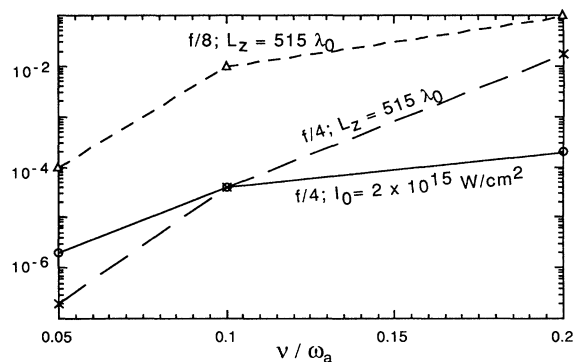


FIG. 4. The reflectivity with $G = 12.5$ [see Eq. (2)] and SSD bandwidth $\Delta\omega = 4 \times 10^{-4} \omega_0$ vs acoustic damping rate ν_a/ω_a for $L_z = 515\lambda_0$ and varying intensity ($f/4$, \times , $f/8$, Δ) and an intensity of 2×10^{15} W/cm² and varying length ($f/4$, \circ).

Rosen for their interest and suggestions. This work was performed under the auspices of the U.S. Department of Energy by the Lawrence Livermore National Laboratory under Contract No. W-7405-Eng-48.

- [1] A.N. Mostovych *et al.*, Phys. Rev. Lett. **59**, 1193 (1987); O. Willi *et al.*, Phys. Fluids B **2**, 1318 (1990); W. Seka *et al.*, Phys. Fluids B **4**, 2232 (1992); C. Labaune *et al.*, Phys. Fluids B **4**, 2224 (1992); J.M. Moody *et al.*, "Beam Smoothing Effects on the Stimulated Brillouin Scattering Instability in Nova Exploding Foil Plasmas" (to be published).
- [2] S.N. Dixit *et al.*, Applied Optics **32**, 2543 (1993); J.W. Goodman, *Statistical Optics* (Wiley, New York, 1985); H.A. Rose and D.F. Dubois, Phys. Fluids B **5**, 590 (1993).
- [3] R.L. Berger *et al.*, Phys. Fluids B **5**, 2243 (1993).
- [4] B. Ya. Zeldovich, N.F. Pipiletsky, and V.V. Shkunov, *Principles of Phase Conjugation* (Springer-Verlag, Berlin, 1985).
- [5] N.E. Andreev and L.M. Gorbunov, JETP Lett. **56**, 144 (1992).
- [6] H.A. Rose and D.F. Dubois, Phys. Rev. Lett. **72**, 2883 (1994).
- [7] M.R. Amin, C.E. Capjack, P. Frycz, W. Rozmus, and V.T. Tikhonchuk, Phys. Rev. Lett. **71**, 81 (1993); Phys. Fluids B **5**, 3748 (1993).
- [8] E.A. Williams *et al.*, Phys. Plasmas **2**, 129 (1995).
- [9] M.D. Feit and J.A. Fleck, J. Opt. Soc. Am. B **5**, 633 (1988).
- [10] T.B. Kaiser *et al.*, Phys. Plasmas **1**, 1287 (1994).
- [11] S. Skupsky *et al.*, J. Appl. Phys. **66**, 3456 (1989).
- [12] D.M. Pennington *et al.*, Tech. Dig. **8**, 161 (1994).
- [13] The pattern would not repeat if the frequency separations were incommensurate.
- [14] L.V. Powers *et al.*, Phys. Rev. Lett. **74**, 2957 (1995).
- [15] B.J. MacGowan (private communication).
- [16] J. Fernandez *et al.*, "Dependence of Stimulated Brillouin Scattering on Laser Intensity, Laser f-number, and Ion Species in Hohlraum Plasmas" (to be published).
- [17] S. Haan *et al.*, "Design and Modeling of Ignition Targets for the National Ignition Facility" (to be published).